CHEMISTRY
A EUROPEAN JOURNAL

DOI: 10.1002/chem.200500731

Internal versus Terminal Metalation of Double-Helical Oligodeoxyribonucleotides

Jo Vinje*[a] and Einar Sletten[b]

Abstract: The formation of adducts between *cis*-$[Pt(NH_3)_2Cl_2]$, Zn^{II}, and Mn^{II} and double-stranded oligodeoxynucleotides was studied by 1D and 2D ^1H, ^{31}P, and ^{15}N NMR spectroscopy. For labile adducts involving Zn^{II} and Mn^{II}, both ^1H chemical shifts (Zn^{II}) and ^1H line-broadening effects (Mn^{II}) showed that in the hexamer $[d(GGCGCC)]_2$ **I**, the terminal G_1-N7 is the exclusive binding site, while for the dodecamer $[d(GGTACCGGTACC)]_2$ **II**, which contains both a terminal and internal GG pair, the preference for metal binding is the internal guanine G_7. Zn^{II} binding to **II** was confirmed by natural-abundance 2D [^1H,^{15}N] HMBC NMR spectroscopy, which unambiguously showed that G_7-N7 is the preferred binding site. The long duplex $[d(GGTATATATACCGGTATA-TATACC)]_2$ **III** was expected to have a more pronounced accumulation of electrostatic potential towards the central part of the sequence (vs the terminal part) than does **II**. However, the Zn^{II} titration of **III** showed no increase in coordination with the internal Gs (vs the terminal Gs), compared with what was observed for **II**. The reaction between the nonlabile metal complex *cis*-$[PtCl_2(^{15}NH_3)_2]$ (cisplatin) and **II** showed a slight preference for the internal GG pair over the terminal GG pair. However, when the diaqua form of cisplatin *cis*-$[Pt(^{15}NH_3)_2(H_2O)_2]$ was reacted with **II** a more pronounced binding preference for the internal GG pair was observed.

Keywords: antitumor agents · DNA · NMR spectroscopy · platinum · zinc

Introduction

Metal ions can bind nucleic acids in two main ways, diffuse and site-binding,[1,2] both of which are important for the structure and function of nucleic acids. In the diffuse binding mode the metal and the nucleic acid retain their hydration layer and the interaction is through water molecules. This is a long-range Coulombic interaction, in which positive metal ions accumulate around the nucleic acid in a delocalized manner; for example, the counter ion atmosphere that all nucleic acids possess is made up of diffuse bound positive ions. In the site-binding mode the metal is coordinated to specific ligands on the nucleic acid; the coordination can either be direct (termed inner-sphere) or through a water molecule (termed outer-sphere). In the outer-sphere binding mode only the innermost hydration layer of the metal is kept intact, and the metal and the nucleic acid ligand(s) to which the metal is coordinated share solvation shells. In inner-shell binding there is direct contact between the metal and the nucleic acid. A dehydration of the metal ion and the nucleic acid binding site therefore has to occur before an inner-shell bond is formed.

The mechanism of inner-sphere binding is likely to be initiated by a diffuse binding mode, in which the metal and the nucleic acid are separated by no more than two layers of solvent molecules.[3] This step is diffusion-controlled. The next step is that the metal ion and the nucleic acid form an outer-sphere complex, separated only by one layer of solvent molecules. This step primarily depends on electrostatic attractions and hydrogen bonding between the metal and the nucleic acid.[4] In the final step the metal and the nucleic acid come into direct contact (inner-sphere binding). Here the nucleophilicity of the coordination site plays a crucial role. In the two last steps steric effects are also important. Several attempts have been made to quantify the importance of accessibility and molecular electrostatic potential

[a] Dr. J. Vinje
Centre of Pharmacy, Department of Chemistry
University of Bergen
Allégt. 41, 5007 Bergen (Norway)
Fax: (+47) 5558-9490
E-mail: jo.vinje@kj.uib.no

[b] Prof. E. Sletten
Department of Chemistry
University of Bergen
Allégt. 41, 5007 Bergen (Norway)

Supporting information for this article is available on the WWW under http://www.chemeurj.org/ or from the author.

(MEP) at the site where the inner-sphere complex/covalent bond is formed.[5–7] In these studies a reasonable correlation between these two important factors has been used to predict the DNA site that is most reactive to metalation or methylation. In the present study we further investigate these effects by looking at double-stranded oligonucleotide sequences containing both a site with high accessibility (terminal GG step) and a site with a more negative electrostatic potential (internal GG step).

A long-term goal is to design metal complexes that can bind selectively to chosen sequences of DNA. Such complexes may be used as drugs that block specific gene expressions associated with a certain disease. Previously, a general selectivity pattern for 3d transition-metal binding to the guanine residues in double-helical oligonucleotides has been proposed, based on proton NMR line-broadening studies and chemical shift measurements.[8–10] The affinity of transition-metal ions for nitrogen N7 of the G-residue on the 5′-side in a double-helical DNA sequence has been shown to follow the order: 5′-GG > GA > GT ≫ GC. Surprisingly, the adjacent residue (X) on the 5′-side (5′-XGG) was found to exert a negligible influence on the selectivity. This sequence-selectivity is *not* observed for single-stranded oligonucleotides (unpublished results). Photoinduced DNA cleavage experiments by Saito et al.[11–13] have shown that the sites in B-form DNA most susceptible toward single-electron oxidation are 5′-residues in 5′-GG-3′ steps. This finding supports our proposed selectivity rule based on NMR experiments.

Previous studies have shown that the electrostatic potential accumulates in the internal part of the oligonucleotides because of Coulombic interaction among nucleic acid phosphates along the backbone.[14–19] This may lead to preferential electrostatic binding of metal ions to the internal part of the oligomer.[20,21] However, since the accessibility of the internal region is not as large as in the terminal part of the double-helical oligonucleotide, metal ions may have a preference for binding to sites in the terminal region of the duplex. A recent X-ray study of Co^{II}, Ni^{II}, and Zn^{II} coordination to the double-helical DNA oligomer $[d(GGCGCC)]_2$ showed only binding to the terminal guanine.[22] The authors concluded that in regular B-DNA conformation the internal binding sites are not accessible to Co^{II}, Ni^{II}, and Zn^{II}, and that consequently these metal ions bind exclusively to the terminal region of double-helical B-DNA, irrespective of base sequence. This is in contrast to our studies, which show a clear sequence-selective binding pattern for 3d metal ions with no special preference for terminal base residues.

In this study we look in more detail at the relative affinity of metalation of internal versus terminal GG pairs in double-helical DNA oligonucleotides. We have used aqua ions of Zn^{II} and Mn^{II}, and compared the binding preference of these ions with that of the antitumour drug *cis*-$[PtCl_2(NH_3)_2]$ (cisplatin). In the latter case the difference in reaction rates between internal and terminal sites were compared using ^{15}N-labeled cisplatin.

Results

Proton assignments of I and II: Both duplexes are self-complementary, and the numbering scheme is as follows, for example, for the hexamer 5′-d($G_1G_2C_3G_4C_5C_6$)-3′: The proton resonances of these sequences were assigned by using the well-known method of sequential connectivity of NOESY cross-peaks for right-handed double-helical DNA, assisted by 2D [^{1}H,^{1}H] TOCSY. The magnitude of the cross-peaks in the NOESY maps of both duplexes indicates normal B-form geometry. The spectra of the imino region exhibit the expected Watson–Crick thymine and guanine imino signals (Figure S1, Supporting Information). This shows that the terminal base pairs do not have any unusual conformation such as extra-helical or extensive base-pair fraying, which are sometimes observed in the terminal base pairs.

Proton assignment of III: Owing to severe overlap of the thymine and cytosine resonances and also the adenine resonances, the spectrum of **III** could not be fully assigned. However, the four guanines were well separated and were assigned from a NOESY map. In addition, the imino-region has 12 imino guanine/thymine signals, which shows that the base pairing is intact throughout the duplex.

Mn^{II} titration: The effects of adding paramagnetic Mn^{II} ions to aqueous solutions of DNA fragments were monitored by observing the decrease in spin–spin (T_2) relaxation times for protons close to the metal centres. Paramagnetic metal ions may be classified according to their electronic correlation times, that is, as relaxation probes producing broad lines or as paramagnetic shift probes with less line broadening. Mn^{II} is a typical relaxation probe with an estimated electronic relaxation time ($t_s = T_{1e} \approx T_{2e}$) of 10^{-8}–10^{-9} s. The line broadening is expressed as line width at half height measured as a function of metal concentration. In kinetically labile metal complexes at low metal-to-nucleotide ratios, paramagnetic shift effects are difficult to detect. In these cases geometric information about metal binding sites are most effectively obtained by measuring proton spin–spin (T_2) relaxation times. Of special interest is the effect on the G-H8 protons adjacent to the expected N7 binding site of guanine residues.

Titration of **I** showed a clear preference for Mn^{II} binding to the G_1 residue, as demonstrated by the plot of line broadening versus $r = [Mn^{2+}]/[\text{duplex}]$ (Figure 1a). A distinct selectivity pattern emerges in which the G_1-H8 signal is appreciably broadened while the G_2-H8 and G_4-H8 signals are only marginally affected.

The Mn^{II} titration procedure was repeated for **II** (Figure 2a). In this duplex there are two GG steps, one terminal (G_1G_2) and one internal (G_7G_8). Figure 2a shows that both of the internal guanines bind Mn^{II}; however, there is a clear preference for the 5′-guanine (G_7) over the 3′-guanine (G_8). The two terminal guanine residues are almost unaffected by the Mn^{II} titration.

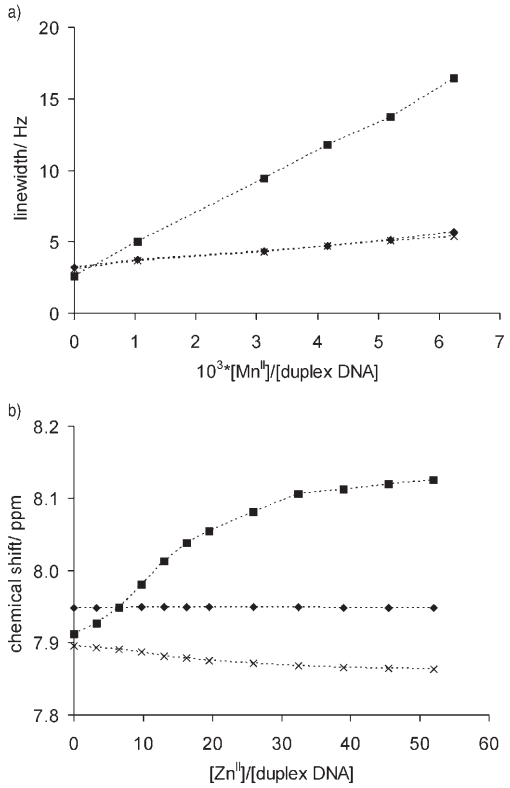

Figure 1. ^{1}H line-broadening and chemical shift measurements for the metal titration of d[(GGCGCC)]$_2$ (10 mM phosphate buffer, 100 mM $NaClO_4$, pH 5.9): ■ = G_1-H8, × = G_2-H8, ◆ = G_4-H8.

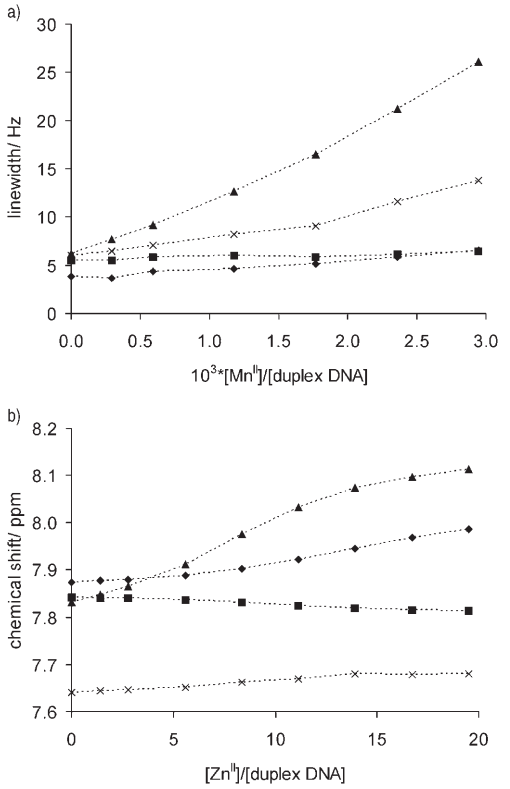

Figure 2. ^{1}H line-broadening and chemical shift measurements for the metal titration of d[(GGTACCGGTACC)]$_2$ (10 mM phosphate buffer, 100 mM $NaClO_4$, in a) pH 6.0 and in b) pH 5.6): ◆ = G_1-H8, ■ = G_2-H8, ▲ = G_7-H8, × = G_8-H8.

Zn^{II} titration: For this diamagnetic system, the variation in chemical shifts for G-H8 protons was monitored as a function of added zinc salt. In contrast to the paramagnetic Mn^{II} system, excess Zn^{II} salt was added to the duplex solutions until an upper limit of metal-ion-induced chemical-shift changes was reached, or until a white precipitate appeared (probably zinc hydroxide or zinc phosphate). The [d-(GGCGCC)]$_2$ duplex shows similar metal-binding selectivity for Zn^{II} as for Mn^{II} (Figure 1b), a clear preference for the G_1-residue. The guanine G_4-H8 signal stays at the same chemical shift value throughout the Zn^{II} titration, while the guanine G_2-H8 signal is shifted 0.03 ppm upfield. The cytosine C_6-H6 and C_3-H6 signals are shifted 0.13 ppm and 0.05 ppm downfield, respectively.

Duplex **II** shows slightly different binding selectivity for Zn^{II} than with Mn^{II} (Figure 2). The most affected signal is G_7-H8, as for the Mn^{II} titration. However, the G_1-H8 signal is relatively more affected than what was apparent in the Mn^{II}-induced line broadening. The G_1-H8 and G_7-H8 signals are shifted downfield 0.1 and 0.3 ppm, respectively; thus there still is a clear preference for the internal GG pair over the terminal one. The two 3′-guanine residues are only slightly influenced; G_2-H8 is shifted 0.03 ppm upfield and G_8-H8 0.04 ppm downfield. The aromatic signals from the other residues are shifted in the range 0.01–0.08 ppm; of these the most affected are C_{12}-H6 (0.08 ppm upfield) and

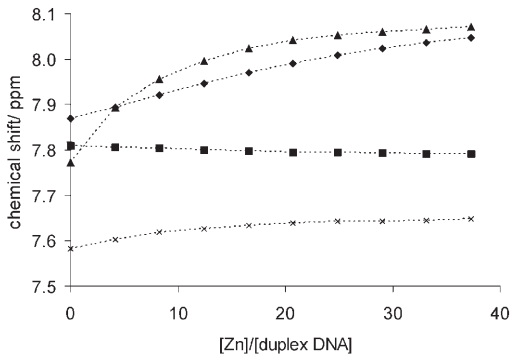

Figure 3. Zn^{II} titration of d[(GGTATATATACCGGTATATATACC)]$_2$ (10 mM phosphate buffer, 100 mM $NaClO_4$ and pH 6.5): ◆ = G_1-H8, ■ = G_2-H8, ▲ = G_{13}-H8, × = G_{14}-H8.

C_6-H6 (0.07 ppm upfield). These cytosines are the complementary bases to G_1 and G_7 and the shifts are therefore most probably a direct result of the Zn^{II} coordination to G_1 and G_7.

A second Zn^{II} titration of **II** was performed at a lower ionic strength; no $NaClO_4$ was added, compared with 100 mM in the previous experiment (Figure S2, Supporting Information). The results of this titration were exactly the same as the one at higher salt concentration, except that a

lower [Zn^{II}]/[duplex DNA] ratio was needed to induce the same chemical shifts as in the high salt experiment.

Zn^{II} titration of **III** was carried out in order to investigate if the expected pronounced accumulation of negative electrostatic potential in the internal region of a long oligonucleotide (compared to shorter ones),[14–19] would lead to a higher selectivity of Zn^{II} binding to the internal GG step, compared with what was observed for **II**. Figure 3 shows the results of the titration, and it is clear that there is no enhanced selectivity for internal Zn^{II} binding. In fact the opposite is observed, as G_1-H8 was now shifted 0.18 ppm and the internal 5′-G-H8 was shifted 0.30 ppm. The two 3′-G-H8 signals were still only slightly shifted.

Natural abundance ^{15}N NMR spectroscopy of II and Zn^{II}/II: In the 2D [^{1}H,^{15}N] HMBC spectra only nitrogen atoms of the purine bases are observed. However, the nitrogen atoms detected in this experiment are known to be the most reactive sites towards relatively soft metal ions like Zn^{II} and Mn^{II}. Therefore the 2D [^{1}H,^{15}N] HMBC spectra shown in Figure 4 unambiguously reveal at which site Zn^{II} ions are coordinated. Figure 5 shows the ^{15}N chemical shift differences of samples with and without added Zn^{II} salt. The G_7-N7 resonance is the most affected signal, being shifted 14.8 ppm upfield. The N7 signals of G_1, G_2, and G_8 are shifted upfield 4.0 ppm, 1.2 ppm, and 1.3 ppm, respectively. The remaining N signals are shifted less than 1 ppm. This correlates well with the ^{1}H chemical shift data (Figure 2b and S2).

Conformational studies of Zn^{II}/II adducts: In order to check conformational changes induced by Zn^{II} coordination to **II**, 2D [^{1}H,^{1}H] NOESY, TOCSY, and E-COSY spectra were recorded for two samples of **II** with and without added Zn^{II}; pH 5.0, 10 mM phosphate buffer, 99.9% D_2O, [Zn^{II}]/[**II**] ratio 0 and 16.8, respectively. In the H8/H6-sugar proton region the sequential walk could be followed; assisted by 2D [^{1}H,^{1}H] TOCSY spectra, this provides an unambiguous assignment of all protons except H5′/H5″. The largest shifts are observed for the sugar protons on residue C_6 (H2′; 0.48 ppm upfield) and (H2″; 0.19 ppm upfield), (Table S1 and Figure S3, Supporting Information). The sugar protons of G_7 are the second most shifted, but these are all shifted downfield (0.14–0.03 ppm). Only minor shifts are observed for the remaining sugar resonances. 2D [^{1}H,^{1}H] E-COSY spectra were used to determine the *J*(H1′,H2′) and *J*-(H1′,H2″) for all residues. (Table S2, Supporting Information).

^{31}P NMR spectra of II and Zn^{II}/II: In 2D [^{1}H,^{31}P] HSQC spectra of DNA oligonucleotides the cross-peaks that are detected involve the phosphate group and sugar protons H3′ (5′-side) and H4′ (3′-side), respectively (Figure 6). The assignment of the phosphate resonances depends on the assignment of the H3′ and H4′ sugar protons, which were assigned from 2D [^{1}H,^{1}H] NOESY and TOCSY. Figure 7 shows the ^{31}P chemical shift difference of the samples with and without added Zn^{II}. The most affected signals are assigned to the phosphate groups connecting residues C_6 and

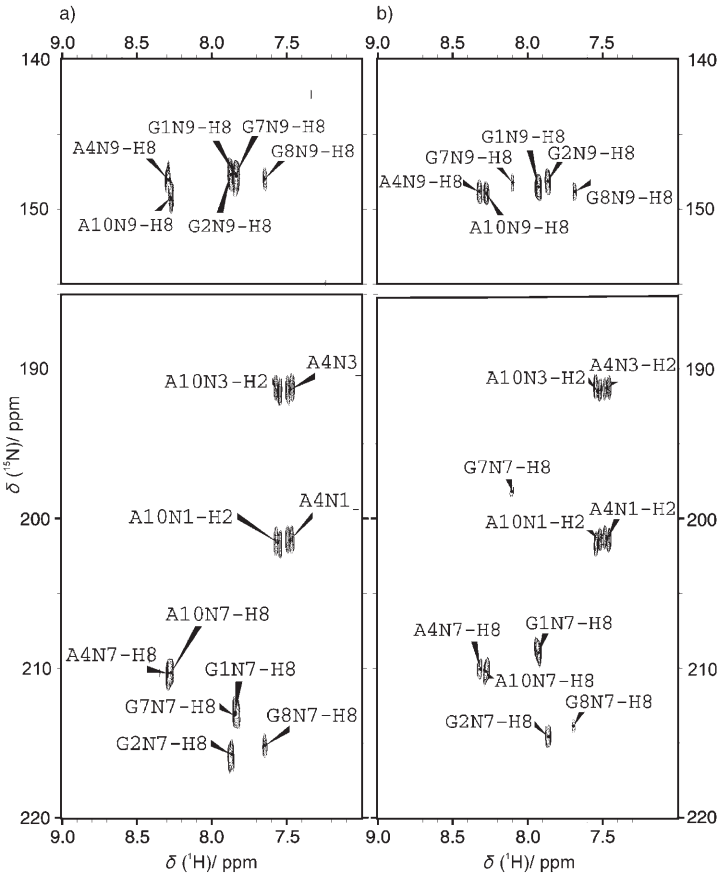

Figure 4. 2D [^{1}H,^{15}N] HMBC NMR spectra. a) 0.29 mM **II** in 10 mM phosphate buffer, pH 5.0, 99.9% D_2O. b) sample as in a) with a Zn^{II}/duplex ratio of 16.8.

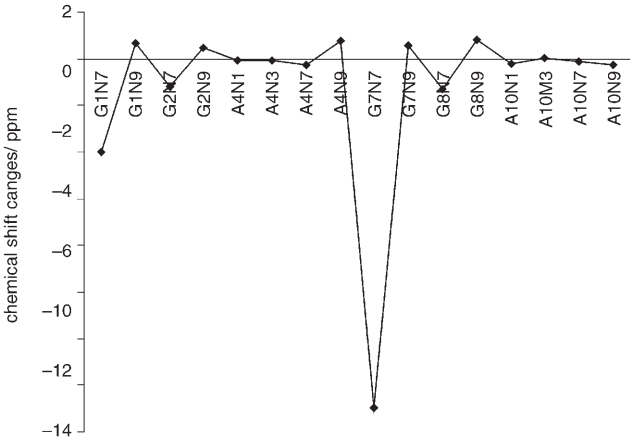

Figure 5. ^{15}N chemical shift differences for the samples: i) 0.29 mM **II** in 10 mM phosphate buffer, pH 5.0, 99.9% D_2O, and, ii) sample as in i) with a Zn^{II}/duplex ratio of 16.8 (measured as δ(ii)-δ(i)).

G_7 (0.60 ppm upfield) and residues G_7 and G_8 (0.51 ppm upfield), respectively. The other ^{31}P resonances are shifted less than 0.1 ppm.

***cis*-[$PtCl_2(^{15}NH_3)_2$] and II**: The reaction could not be fully analyzed by 2D [^{1}H,^{15}N] HSQC NMR owing to overlap of

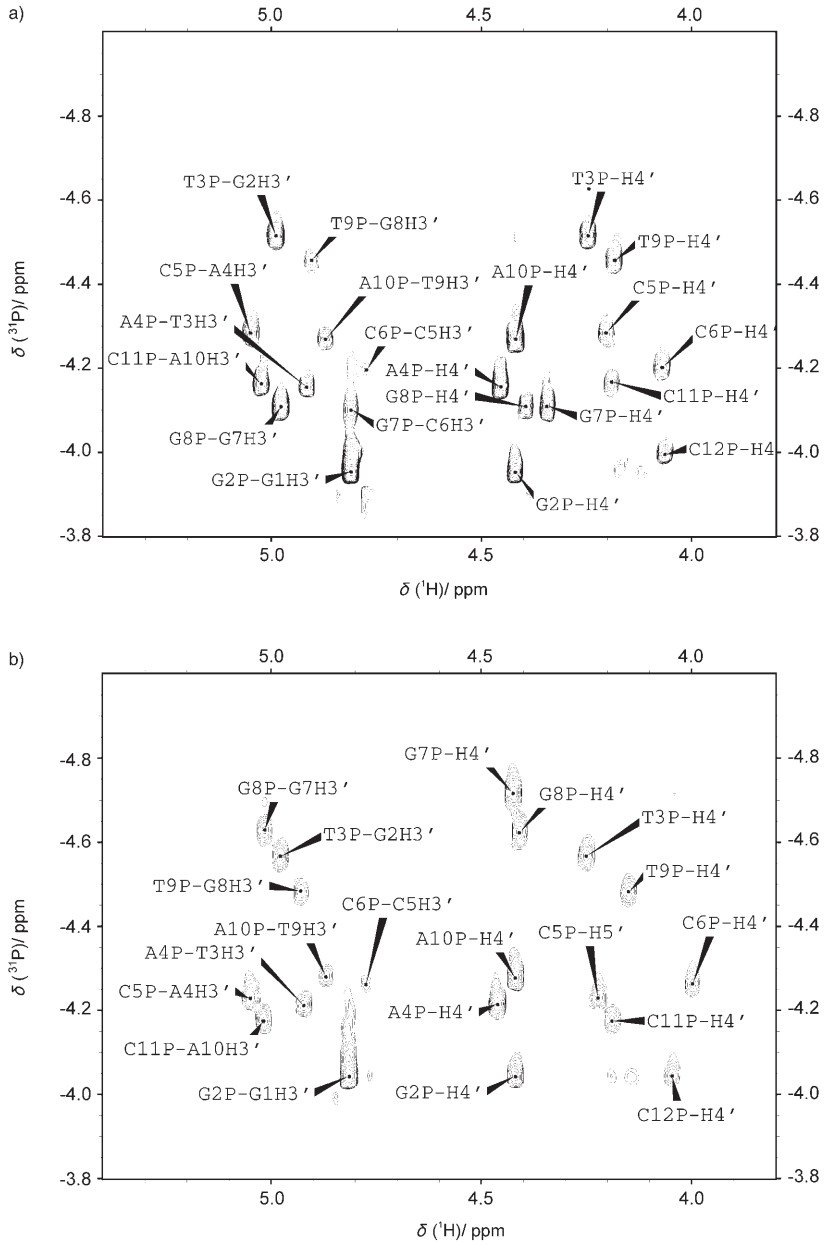

Figure 6. 2D [^{1}H,^{3}P] HSQC NMR spectra. a) 0.29 mM **II** in 10 mM phosphate buffer, pH 5.0, 99.9% D_2O; b) sample as in a) with a Zn^{II}/duplex ratio of 16.8.

the resonances representing the monofunctional adducts (*cis*-[PtCl($^{15}NH_3$)$_2${N7G}]$^+$) and the water signal. Different pH levels and temperatures (pH 5–7 and 285–298 K) were tried to avoid overlap, but this was not successful. However, on the basis of a 2D [^{1}H,^{1}H] NOESY experiment recorded before the reaction was completed (~1 d reaction time, 298 K) it was possible to make an unambiguous assignment of *cis*-[PtCl($^{15}NH_3$)$_2${N7G$_1$}]$^+$ based on the fact that G_1-H8 has only cross-peaks to its own sugar protons H2′/H2″ while the other G-H8 have two additional cross-peaks in the aromatic H2′/H2″ region. Table 1 gives δ(^{1}H)/δ(^{15}N) for all Pt^{II} species observed in this work, and also shows the labelling used for the different species.

In the reaction, signals representing the monoaquated species *cis*-[PtCl($^{15}NH_3$)$_2$(H_2O)]$^+$ (**2**) were not observed (pH 6.0 and 298 K), which indicates that the rate of formation of *cis*-[PtCl($^{15}NH_3$)$_2${N7G}]$^+$ is fast. This is expected since **II** has four "hot spots" for the cisplatin reaction (the GG steps). The signals clearly observed were assigned to *cis*-[$PtCl_2$-($^{15}NH_3$)$_2$] (**1**) at δ(^{1}H)/δ(^{15}N) = 4.07/−69.03 ppm and to two intrastrand crosslinked (CL) adducts (end-products of the reaction) at δ(^{1}H)/δ(^{15}N) = 4.17/−69.18, 4.49/−69.92 ppm (**9**) and 4.46/−67.99, 4.38/68.60 ppm (**10**). These CL adducts were assigned by 2D [^{1}H,^{1}H] NOESY experiments (Figures S4 and S5, Supporting Information), and found to correspond to *cis*-[Pt-($^{15}NH_3$)$_2${N7G$_7$,N7G$_8$}]$^{2+}$ (**9**) and *cis*-[Pt-($^{15}NH_3$)$_2${N7G$_1$,N7G$_2$}]$^{2+}$ (**10**). In the NOESY maps the two adducts could easily be assigned from their strong G*-H8···G*-H8 (G* indicates platinated guanine) cross-peaks, showing that both had a head-to-head conformation,[23] which has also been found in all published duplex *cis*-[Pt($^{15}NH_3$)$_2$-{N7G,N7G}]$^{2+}$ intrastrand complexes.[24–30]

In all duplex intrastrand cisplatin GG adducts one observes the 5′-G*-H8 signal shifted downfield (~8.7 ppm) of the 3′-G*-H8 signal (δ = 8.0–8.4 ppm).[24–30] Based on this fact, the most downfield shifted G*-H8 in each adduct was considered to be either G_1*-H8 or G_7*-H8. On the basis of this assumption, the two 5′-G*-H8 resonances could be distinguished in the aromatic-H2′/H2″ region of the NOESY maps; since G_1 is the terminal 5′-residue in **II**, G_1*-H8 will only have cross-peaks to its own sugar protons, thus only two cross-peaks in the aromatic H2′/H2″ region. On the other hand G_7*-H8 will also have cross-peaks to the sugar protons on its 5′ neighbouring residue (C_6) and will therefore have four cross-peaks in the aromatic H2′/H2″ region. The same holds for the aromatic H1′ and aromatic H3′ regions, in which G_1*-H8 only has a single cross-peak, while G_7*-H8 shows two cross-signals in each

Table 1. ^{1}H and ^{15}N NMR chemical shift values and numbering for cisplatin species involved in the reactions with **II**.[a]

Species		$\delta(^{1}H)/\delta(^{15}N)$	*trans* ligand
cis-$[PtCl_2(NH_3)_2]$	**1**	4.07/−69.03	Cl
cis-$[PtCl(H_2O)(NH_3)_2]^+$	**2**	not observed	
cis-$[Pt(^{15}NH_3)_2(H_2O)_2]^{2+}$	**3**	3.84/−81.55[b]	O
cis-$[Pt(^{15}NH_3)_2(H_2O)(OH)]^+$	**4**	3.84/−81.55[b]	O
cis-$[Pt(^{15}NH_3)_2(OH)_2]$	**5**	3.84/−81.55[b]	O
cis-$[Pt(^{15}NH_3)_2(OH)\{N7G_7/N7G_8\}]^+$ no 1	**6**	4.26/−68.55[c]	N
	6	3.78/−82.05[c]	O
cis-$[Pt(^{15}NH_3)_2(OH)\{N7G_7/N7G_8\}]^+$ no 2	**7**	4.07/−67.26[c]	N
	7	4.01/−77.07[c]	O
cis-$[Pt(^{15}NH_3)_2(OH)\{N7G_1/N7G_2\}]^+$	**8**	4.26/−68.43[c]	N
	8	3.94/−78.27[c]	O
cis-$[Pt(^{15}NH_3)_2\{N7G_7,N7G_8\}]^{2+}$	**9**	3.80/−71.03	N
	9	3.86/−71.39	N
cis-$[Pt(^{15}NH_3)_2\{N7G_1,N7G_2\}]^{2+}$	**10**	3.89/−72.81	N
	10	3.92/−73.65	N

[a] Chemical shift values are given for the species at 298 K and pH 6.0 unless otherwise stated. All samples contain 100 mM $NaClO_4$. [b] These species are indistinguishable in the NMR spectra owing to fast exchange. $T = 285$ K and pH 7.2–7.3. [c] $T = 285$ K and pH 7.4–7.5.

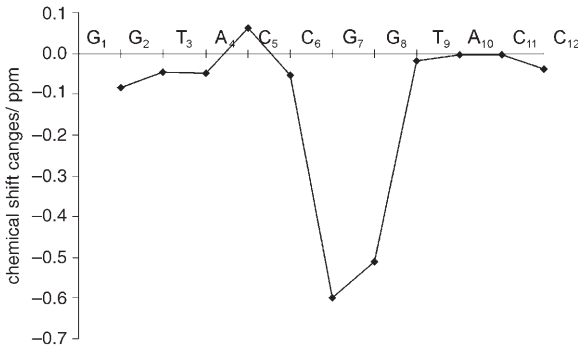

Figure 7. ^{31}P chemical shift differences for the samples: i) 0.29 mM **II** in 10 mM phosphate buffer, pH 5.0, 99.9% D_2O; ii) sample as in i) with a Zn^{II}/duplex ratio of 16.8 (measured as δ(ii)−δ(i)).

region. The assignment of the 3′-G*-H8 signals in **9** and **10** were confirmed by the cross-peak between 3′-G*-H8 and the methyl group on thymine (G_2*-H8···T_3-Me and G_8*-H8···T_9-Me), which excludes the possibility that these resonances correspond to 5′-G*-H8.

Other features in the NOESY maps that support the assignments are a strong G_7*-H8···H3′ cross-peak and the fact that the G_7*H3′ resonance is the most downfield shifted H3′ resonance. In contrast, the G_8*-H8···H3′ cross-peak is not especially strong, nor is it shifted downfield. In all duplex structures of intrastrand cisplatin adducts a strong 5′-G*H8···H3′ cross-peak and downfield shift of 5′-G*H3′ were observed, indicating that the sugar on the 5′-G* has N-type conformation while the sugar on the 3′-G*-side retains the usual *S*-type conformation.[23] In **10** such an intense G*-H8-H3′ cross-peak is not observed, and none of the G*-H3′ signals are shifted significantly downfield. This suggests that the conformation of the terminal adduct is slightly different from that of the internal adduct.

The ratio between **9** and **10** was 1.6:1 when **II** was treated with cisplatin in equimolar amounts, and 1:1 when the reaction was performed at **II**/cisplatin ratio of 1:2. The two adducts were seen to be stable for weeks and the ratio between them remained constant.

***cis*-$[Pt(^{15}NH_3)_2(H_2O)_2]^{2+}$ and II**: The reaction was carried out at pH 6.4 and 285 K. The low temperature and relatively high pH were used in order to slow the reaction down to a rate that could be followed by 2D $[^{1}H,^{15}N]$ HSQC NMR spectroscopy. During the reaction the pH increased to a final value of 8.2. At this pH *cis*-$[Pt(^{15}NH_3)_2(H_2O)_2]^{2+}$ (**3**) exists mainly in its deprotonated forms, *cis*-$[Pt(^{15}NH_3)_2(H_2O)(OH)]^+$ (**4**) and *cis*-$[Pt(^{15}NH_3)_2(OH)_2]$ (**5**) ($pK_{a1} = 5.37$, $pK_{a2} = 7.21$).[31] The chemical shifts of the protons of the ammine group on Pt^{II} depend on the *trans* ligand (H_2O or OH^-), and thus the shift of the ammine groups may be used to determine the pH of the sample. ^{1}H and ^{15}N calibration curves were determined by titrating a sample of **3** (0.5 mM, pH 5.5, 0.1 M $NaClO_4$, 285 K) with NaOH in a series of 2D $[^{1}H,^{15}N]$ HSQC NMR experiments (data not shown). From the regression curves of the pH titration of **3**, the pH evolution during the reaction between **3** and **II** can be estimated (Figure S6, Supporting Information). From the plot we can see that after about 40 minutes the pH has increased from 6.4 to 7.4, which shows that a large fraction of **3**/**4** has been transformed into **5**. Since the dihydroxo form **5** is assumed to be much less reactive than **4**, the latter is probably the reactive species. Species **4** may also be the species reactive towards DNA in vivo, depending on the time that cisplatin has to equilibrate with the internal environment of the cell (assuming an intracellular environment of pH 7.4 and [Cl] ~10 mM).

In the 2D $[^{1}H,^{15}N]$ HSQC spectra the $^{15}NH_3$ groups of cisplatin with H_2O or OH^- in the *trans* position will appear upfield in the ^{15}N dimension compared to the ones having G-N7 or chloride in the *trans* position.[32] It is not possible to distinguish between **3**, **4**, and **5** based on $^{15}NH_3$ shifts owing to the fast exchange of H^+ on the NMR time scale. Figure 8 shows a 2D $[^{1}H,^{15}N]$ HSQC NMR spectrum of the reaction mixture after 4.5 h reaction time.

One may distinguish between mono- and bifunctional G-N7 adducts from the fact that the intensity of the peaks due to the former decreases towards the end of the reaction. Moreover, only the chemical shifts of the monofunctional adducts are influenced by the change in pH that occurs during the reaction. The (G_7-N7,G_8-N7) CL **9** was assigned from 2D $[^{1}H,^{1}H]$ NOESY spectra. This assignment was confirmed by the fact that the $^{1}H/^{15}N$ shift of **9** at 297 K (4.16/−69.06, 4.46/−69.78) is the same as that found for **9** in the reaction between **1** and **II** at 298 K (Table 1). The CL adduct of the terminal guanines (G_1-N7,G_2-N7) **10** could not be assigned from 2D $[^{1}H,^{1}H]$ NOESY spectra owing to the low concentration of this species. However, the adduct has the same chemical shift in the 2D $[^{1}H,^{15}N]$ HSQC spectra at

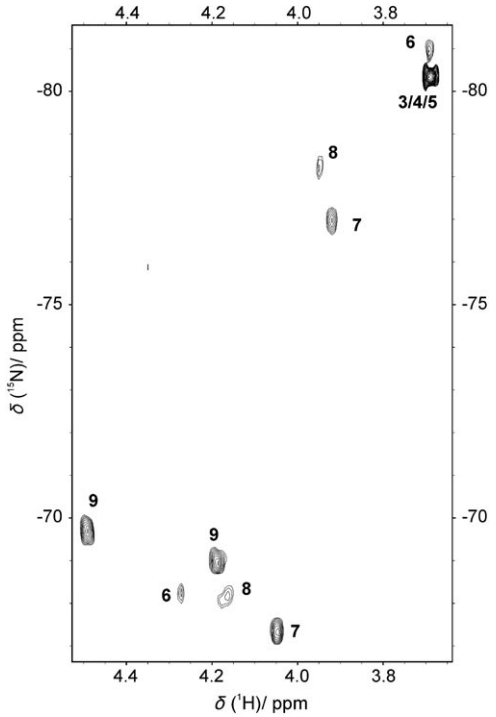

Figure 8. 2D [^{1}H,^{15}N] HSQC NMR spectrum of the reaction starting with 0.59 mM of *cis*-[Pt(^{15}NH$_3$)$_2$(H$_2$O)$_2$]$^{2+}$ (**3**) and 0.59 mM of **II** (100 mM $NaClO_4$, pH 7.8–7.9, 285 K). This spectrum was recorded after 4.5 h reaction time. The labelling is as used in Table 1.

297 K (δ(^{1}H)/δ(^{15}N) = 4.43/−68.05, 4.38/−68.38 ppm) as the shifts found for **10** in the reaction between **1** and **II** at 298 K (Table 1).

The monofunctional internal guanine adducts were distinguished from the terminal guanine adducts by comparing their relative intensities. Since the intensities of the former reach a maximum higher than the final concentration of the (G_1-N7, G_2-N7) CL adduct **10**, an unambiguous distinction could be made. However, it was not possible to determine whether monofunctional platination takes place at one or both of the internal Gs. The monofunctional adduct of the terminal Gs was assigned on the basis of its low concentration, and how its concentration evolves. Whether the site of platination is G_1 or G_2 could not be determined.

After about 22 h one of the monofunctional adducts of the internal guanines and the terminal monofucntional adduct disappeared. After 23 h a pair of peaks at δ(^{1}H)/δ(^{15}N) = 4.41/−68.30 and 4.46/−67.78 ppm appears (assigned **10**), and after 61 h the signal from **4/5** is no longer visible. After the reaction had continued for 66 h, the temperature was raised to 297 K. Five hours after the temperature was increased the second monofunctional adduct of the internal guanines disappeared, and at this time only the signals from **9** and **10** were visible. The ratio of the two adducts measured four days after the reaction was initiated was 6.5:1 (**9**:**10**).

Figure 9 shows the concentration curves for the reaction of fully aquated cisplatin and **II**. Table 2 gives the corresponding optimized rate constants. In the kinetic model a

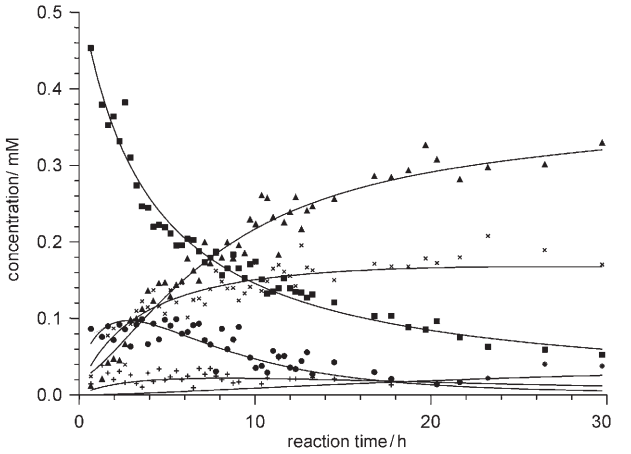

Figure 9. Experimental concentrations (from NMR spectra) and theoretically fitted curves for the reaction starting with *cis*-[Pt(^{15}NH$_3$)$_2$(H$_2$O)$_2$]$^{2+}$ (**3**) and **II** (100 mM $NaClO_4$, pH 6.4–8.2, 285 K): ■ = **3/4/5**, ● = **6**, × = **7**, + = **8**, ▲ = **9**, * = **10**.

Table 2. Platination rate constants (standard deviation in parentheses) for the reaction starting with *cis*-[Pt(^{15}NH$_3$)$_2$(H$_2$O)$_2$]$^{2+}$ and **II** (285 K, pH 6.4–8.2 and 100 mM $NaClO_4$).

Rate constants	
k_1[a]	0.074 (5) $M^{-1}s^{-1}$
k_2[b]	0.053 (5) $M^{-1}s^{-1}$
k_3[c]	0.011 (1) $M^{-1}s^{-1}$
k_{c1}[d]	7.0 (3) $s^{-1}\times10^{-5}$
k_{c2}[e]	0.14 (8) $s^{-1}\times10^{-5}$
k_{c3}[f]	1.4 (6) $s^{-1}\times10^{-5}$

[a] Rate of formation of **6**. [b] Rate of formation of **7**. [c] Rate of formation of **8**. [d] Rate of formation of **9** from **6**. [e] Rate of formation of **9** from **7**. [f] Rate of formation of **10** from **8**.

second-order reaction between **3/4/5** and **II** is assumed to form the monofunctional adducts, and the CL step is considered as a first-order reaction from the monofunctional adduct. The two rate constants for the formation of the monofunctional adducts of the central guanines are 5–7 times faster than for the terminal guanines. Another interesting feature is that one of the two monofunctional adducts of the central guanines was stable for a long time (~3 d). The rate of CL formation in this adduct was about 50 times lower than in the second monofunctional adduct of the central guanines and 10 times lower than in the terminal monofunctional adduct.

Discussion

Binding sites for Zn^{II} and Mn^{II} in I and II: Sigel and coworkers have published an extensive series of potentiometric measurements on metal-ion binding to nucleotides.[33,34] They conclude that the predominant binding pattern for 3d metal ions such as Zn^{II} and Mn^{II} can be described as a mac-

rocyclic chelate in which the metal ion forms inner-sphere bonds both to phosphate and to a heterocyclic nitrogen. The high affinity found for metal ion binding to the phosphate group of nucleoside monophosphates may be explained by the twofold negative charge on the phosphate group. In oligonucleotides the phosphate group is replaced by a phosphodiester, which has only one negative charge and is also less basic than monophosphate monoester residues. Sigel's group recently reported that M^{II} binding to GG dinucleoside monophosphates occurs predominantly by coordination to N7 on the 5′-G, and that no inner-sphere coordination to the phosphodiester group is present in the complex (in contrast to earlier results for nucleoside monophosphates).[35]

The ^{1}H, ^{15}N, and ^{31}P NMR spectroscopic results for the reaction of **II** with Zn^{II} may be interpreted as follows: the downfield ^{1}H shifts of G_1-H8 (0.1 ppm) and G_7-H8 (0.3 ppm) (Figure 2b) indicate preference for binding at the internal G_7 rather than the terminal G_1-site. This interpretation is fully supported by Zn^{II}-induced $^{15}N7$ chemical shifts for G_7-N7 (14.8 ppm upfield) and G_1-N7 (4.0 ppm upfield) (Figures 4 and 5). An upfield ^{15}N shift of 12.2 ppm has been calculated for inner-sphere Zn^{II} coordination to G-N7,[36] and an experimentally determined G-N7 upfield shift of ~20 ppm has previously been reported.[37,38] The consistently lower proton and nitrogen chemical shift changes of G_1 versus G_7 show that the interior site has higher affinity for metal coordination than the terminal site. From the discussion above it is clear that the 1D ^{1}H shift data from the titration of **II** with Zn^{II} are in agreement with the 2D [^{1}H,^{15}N] HMBC NMR data (Figures 2b and 4). Thus, ^{1}H shift data give a true picture of where Zn^{II} is coordinated, so the ^{1}H shift data obtained by titration of **I** with Zn^{II} may also be assumed to show where Zn^{II} is coordinated. Figure 1b shows clearly that Zn^{II} coordinates exclusively to G_1-N7 in **I**.

These observations disagree completely with the hypothesis, based on X-ray structures of DNA oligonucleotide transition-metal complexes, that in standard B-form DNA, Zn^{II} binds exclusively to the terminal region of the duplex, regardless of base sequence.[22,39] On the basis of the X-ray structure of the Ni^{II} complex of $[d(CGTATAACG)]_2$, the authors also concluded that Ni^{II} cannot bind to guanines in standard B-form DNA.[40] The three papers refer to work done by Gao et al.,[41] in which different models of Co^{II} coordinated to G-N7 in 5′-XGY-3′ (X, Y = A, G, C, or T), with the triplet sequences in B-DNA conformation, were studied. The models show that there is always a short contact between one of the Co^{II} aqua ligands and the base on the 5′-side, while the 3′-side is unrestrained. The authors conclude that when Co^{II} is bound to a guanine base of B-DNA, either Co^{II} has to lose some of its octahedral hydration shell or a conformational change must occur in the adjacent position. The authors also suggest that such a conformational change (e.g. change in helical twist angle) may occur in solution, however in a crystal lattice this conformational change may not be feasible. Thus, from our solution studies and the X-ray structures,[22,39,40] there appears to be a difference between the binding preference of transition-metal ions in crystal lattices and solutions. This difference may be explained by the model studies done by Gao et al.[41]

The question concerning inner versus outer sphere phosphate coordination has usually been discussed in relation to mono- or dinucleotide binding. Marzilli et al. have shown that direct $Pt{-}PO_4$ binding to IMP produces a ^{31}P downfield shift of about 3.5 ppm.[42] The same group has reported a ~1 ppm (^{31}P) downfield shift of the phosphodiester group on binding of different Pt^{II} amines to G-N7 in DNA oligonucleotides.[43] The shift was shown to depend on base sequence (especially if there was a phosphate group next to the 5′-G) and type of Pt^{II} complex. This chemical shift change is due to conformational changes of the phosphodiester backbone and shows how sensitive the ^{31}P NMR signals are to conformational changes. The authors indicate that exchanging one of the aqua ligands hydrogen bound to the phosphodiester group by hydrogen bonding to an amine group shifts the ^{31}P signal by no more than 0.1 ppm.

In the reaction of *cis*-$[Pt(NO_3)(NH_3)_3]^+$ and *cis*-$[Pt(NO_3)_2(NH_3)_2]$ with $d(TpT)^-$ in *N*,*N*-dimethylformamide (DMF), the phosphate group is shifted 8 ppm downfield.[44] In this case Pt^{II} coordinates directly to phosphate oxygen and not to the thymine bases. When $d(TpT)^-$ was replaced by $d(TpG)^-$, a ^{31}P upfield shift of 1 ppm in addition to a 1.1 ppm downfield shift of G-H8 were observed in accordance with the expected direct coordination of Pt^{II} to G-N7 and no binding to the phosphate group. In conclusion, direct coordination of Pt^{II} to phosphate oxygen induces a ^{31}P shift of several ppm units, while coordination to G-N7 and no direct binding to phosphate oxygen induces a shift of around 1 ppm. This has also been reported in other studies.[45–47]

An example of chemical shift changes induced by direct coordination of M^{II} aqua ions to phosphate oxygen is reported in a titration of fully ionized ATP with Mg^{II}; here ^{31}P downfield shifts in the 2.1–3.3 ppm range are reported.[48]

In the present case of **II**, the largest ^{31}P chemical shift differences are associated with the central residues C_6pG_7 (0.60 ppm upfield) and G_7pG_8 (0.51 ppm upfield). These shifts must be caused either by hydrogen bonding between the water ligands coordinated to Zn^{II} and the phosphodiester group, or conformational changes in the duplex induced by metalation. According to Gao et al. (see above), coordination of an octahedral M^{II} aqua complex to G-N7 should induce conformational changes on the adjacent base pairs. On the other hand, changing the environment of phosphate oxygen from $Na^+{-}OH_2{-}OPO_3$ to $Zn^{II}{-}OH_2{-}OPO_3$ should not induce a significant shift of the ^{31}P resonance (according to ref. [43], see above). Thus, it is most likely that the observed ^{31}P shift changes of C_6pG_7 and G_7pG_8 are due to conformational changes to accommodate the aqua ligands of Zn^{II} at the G_7-N7 site.

In the Mn^{II} titration of **I** and **II**, the concentration of Mn^{II} is about one thousand times less than the duplex concentration. Mn^{II} is paramagnetic, and functions as a typical relaxation probe. The metal ion produces significant line broadening of the NMR signals at the site of interaction, even at a very low ratio of Mn^{II} to DNA. In this case it is unlikely

that the duplex conformation is perturbed and the line broadening of the G-H8 signals (Figures 1a and 2a) therefore directly show where the metal is coordinated.

Conformation of the Zn^{II}/II adduct: ^1H chemical shift changes induced by Zn^{II} coordination to **II** (Table S1, Supporting Information) show that the conformation of **II** is perturbed. The largest shifts are observed for the sugar protons on residue C_6 (H2′; 0.48 ppm upfield) and (H2″; 0.19 ppm upfield). In the NMR structures of intrastrand 1,2-GG cisplatin duplex DNA adducts, a significant upfield shift of H2′ (~0.5 ppm) on the residue X adjacent to the 5′-G (5′-XGG-3′, X = T or C) has been observed.[24–30] This chemical shift has been explained by a movement of 5′-G towards the outside of the duplex (a positive slide), which brings XH2′ into the shielding cone of 5′-G.[49]

Another characteristic feature observed in intrastrand 1,2-GG cisplatin duplex DNA adducts is the conformational change of the sugars of the platinated site. Generally, a shift of predominant S conformation to a predominant N conformation is observed for the two residues 5′-XG*.[24–30] In order to check whether such a conformational change occurs in the Zn^{II} adduct of **II**, the H1′–H2′and H1′–H2″ coupling constants were determined. In the pure duplex all J(H1′,H2′) > J(H1′,H2″), which shows that all have a higher percentage *S* conformation (Table S2, Supporting Information). When Zn^{II} is coordinated to **II** all J(H1′,H2′) > J(H1′,H2″), except for residue C_6; here J(H1′,H2″) are 0.8 Hz larger than J(H1′,H2′). This indicates that the percentage of N conformation is slightly higher than S for the sugar on residue C_6. Thus, the E-COSY data shows that a conformational change of the sugar unit occurs on the 5′-side of the metalated guanine.

The ^{31}P shift data show that the phosphate groups, one on each side of the site of Zn^{II} coordination, are most shifted; C_6pG_7 (0.60 ppm upfield) and G_7pG_8 (0.51 ppm upfield), see Figure 7. This indicates that a change in the phosphodiester backbone conformation has occurred. However, the shifts are not as dramatic as those observed in intrastrand 1,2-GG cisplatin duplex DNA adducts,[24–30] and the perturbation of the backbone is therefore considered to be minor.

Zn^{II} does not form a 1,2-GG crosslinked adduct like cisplatin; earlier studies by our group have shown it to bind monofunctionally (inner-sphere) to G-N7.[8–10] The 2D [^1H,^{15}N] HMBC NMR spectra of the Zn^{II}/II adduct (Figures 4 and 5) also show that only one G-N7 in each GG pair is shifted, clearly indicating that no crosslink is formed. However, it is likely that the aqua ligands of the Zn^{II} ion coordinated to G-N7 makes hydrogen bonds to neighbouring bases or to phosphate on the phosphodiester backbone. The Zn^{II}/**II** adduct may be similar to that observed for monofunctional Pt adducts, for example, duplex adducts of *trans-EE*, $[PtCl(NH_3)_3]^+$ or $[PtCl(dien)]^+$.[10,50–53] However, Zn^{II} is a labile metal ion and comparison with the inert Pt^{II} complexes is therefore not straightforward.

Factors determining the binding preference of Zn^{II} and Mn^{II} to I–III: The Zn^{II} and Mn^{II} titration results for **I** show exclusive binding to the terminal 5′G residue (Figure 1). This is in accordance with our previously proposed rule for sequence selectivity, where the affinity follows the order: 5′-*G*G > *G*A > *G*T ⋙ *G*C.[8–10] Figure 2 shows the ^1H NMR spectroscopic results for the titration of **II** by Mn^{II} and Zn^{II}. The binding of Zn^{II} and Mn^{II} is seen to qualitatively follow the proposed selectivity rule, 5′*G*GT > 5′G*G*T. The apparent difference between Zn^{II} and Mn^{II} binding to the terminal GG pair (less Mn^{II} coordinates to the terminal GG step than what is found for Zn^{II}) may be related to differences in titration conditions: the concentration of Mn^{II} is a thousand times lower than the concentration of **II**, while in the Zn^{II} titration there is a tenfold excess of Zn^{II}, which may produce a different screening effect on negative electrostatic potentials. Another explanation may simply be that as more Zn^{II} coordinates to G_7-N7 throughout the titration, fewer G_7-N7 sites are available for Zn^{II} binding, and therefore Zn^{II} starts to coordinate at G_1-N7. The chemical shift data of the reaction at a ratio of 3:1 ([Zn^{II}]/[**II**]) give a G_7-H8/G_1-H8 ratio of 6:1. The final ratio of the chemical shift G_7-H8/G_1-H8 for the titration is 3:1, indicating that the preference for the internal guanines is higher at low [Zn^{II}]/[**II**]. It may therefore be that Zn^{II} has a binding preference similar to that of Mn^{II} under the conditions in which the Mn^{II} titration was performed. The most convincing evidence for sequence-selective Zn^{II} binding is presented in Figure 4, in which natural-abundance ^{15}N NMR spectra of **II** clearly show direct Zn^{II}-N7 interaction at G_7 and to a lesser degree G_1, which quantitatively also agrees well with the ^1H spectroscopic results (Figures 2b and S2).

To what extent do electrostatic interactions originating from the phosphate backbone influence sequence-selective metalation of double-helical oligonucleotides? Several groups have dealt with this question, but mainly by using single-strand model systems. In our approach we look at two different factors: 1) the effect of using a lower counterion concentration, and 2) the influence of the length of the oligomer. Theoretical calculations by Lavery et al. indicate that the electrostatic potential of double-stranded DNA oligonucleotide accumulates in the central part of the DNA oligonucleotide; in the calculation the effects of both the phosphate groups and the nucleobases were taken in to account.[54] For single-strand systems it has been shown that metal binding tends to accumulate in the interior of the sequences.[14–19] This effect is referred to as the Coulombic end effect (CEE), and it has been shown to be greater at low ionic strengths and for longer oligonucleotides. In reference [16] CEE was shown to increase for single-stranded oligonucleotides of up to at least 69 residues in length.

In order to test whether CEE is the factor that can account for the preference of Zn^{II} coordination to the internal GG step, the Zn^{II} titration of **II** was repeated for a sample in which the salt concentration was decreased from 0.1 M $NaClO_4$ to none, in order to observe the expected reduction in preference for the terminal GG step. However, it was

shown that the preference for the two GG steps in the Zn^{II} titration at zero $NaClO_4$ is equal to the one performed at 0.1 M $NaClO_4$ (Figures 2b and S2, Supporting Information). Since the CEE is also dependent on the length of the oligonucleotides, a Zn^{II} titration of a 24 base pair long duplex (**III**) was performed. The titration shows that the ratio of internal to terminal G coordination is less for **III** than for **II** (Figures 3 and 2b); this is contrary to what was expected.

Recent studies of Pt^{II} coordination to single-stranded oligonucleotides of variable length and different salt conditions have indicated that CEE is a major factor in determining the rate of an electrostatic pre-association step between Pt^{II} and single-stranded oligonucleotides.[20,21] CEE was therefore considered to be a major factor for the rate of platination of single-stranded DNA oligonucleotides. The Zn^{II} titration results for **II** and **III** in this paper show that CEE is not as dominant for the metal-binding preference in double-helical DNA oligonucleotides as it is in single-stranded DNA oligonucleotides. At least, the same predictions that come from CEE to explain the reactivity of single-stranded DNA oligonucleotides cannot be used for double-stranded DNA oligonucleotides. A major difference between single-stranded and double-stranded DNA is the stacking interactions found in double-stranded DNA, which are absent, or at least less significant, in single-stranded DNA. One important effect from stacking interactions is the ability of orbitals to delocalize between the stacked bases. Calculations made by Saito et al. have shown that the HOMO of two stacked GG pairs has especially high energy and is mainly localized on the 5′-G.[11–13] The calculations also show that the localization of the HOMO is dependent on the neighbouring bases of the GG step and the conformation of the duplex. Certain base sequences therefore become especially reactive towards oxidation or electrophilic attack. The metalation selectivity found in **I**, **II**, and **III** fits qualitatively with predictions based on these HOMO calculations. However, in order to explain the distinct binding preference of Zn^{II} and Mn^{II} for the internal GG step in **II** and **III**, electrostatic effects such as CEE and the calculations done by Lavery et al. have to be invoked.[14–19,54]

Cisplatin metalation of II: The binding preference for internal versus terminal GG pairs in the reaction starting with **3** and **II** is 6.5:1, while in the reaction starting with **1** and **II** the ratio is 1.6:1. The fact that both Pt^{II} species prefer the internal GG step is very interesting, and shows that steric effects in the binding mechanism of cisplatin to double-stranded DNA are not a major factor. In a recent paper the rate of platination of double-stranded DNA was predicted to be proportional to the accessibility of the G-N7 van der Waals surface.[7] This accessibility was shown to be hindered by neighbouring residues on both the 5′-side and the 3′-side. The terminal guanine in **II** should therefore have exceptionally favourable accessibility, considerably favouring platination of this site over the internal GG step. Since platination predominantly occurs on the internal GG step, steric effects cannot be such a major factor as suggested in ref. [7] and also proposed in other studies.[5,55] This is an important observation in relation to the design of new platinum drugs, for which side-effects may be reduced and cisplatin resistance overcome through more sterically fine-tuned, hindered platinum complexes. This may be achieved by introducing bulky groups on the platinum centre, thereby reducing reactivity towards unwanted biomolecules.[56,57] The results of this study show that cisplatin does not contain ligands that induce a significant steric hindrance for reactivity with DNA. On the contrary, we have recently shown that a promising antitumour *trans*-Pt^{II} complex, containing bulky iminoether groups, only reacts with terminal guanines in double-stranded DNA.[58]

In the reaction starting with **1** and **II** (pH 6.0), species **2** will be the reactive species,[59–61] while in the reaction starting with **3** and **II** (pH 6.4–8.2) the reacting species is **4**. This can be rationalized from the fact that the reaction mainly evolves at a pH above pK_{a2} 7.21 of **3**[31] and at this pH the most abundant species is **5**. However, hydroxide is such a poor leaving group that **5** is basically nonreactive compared with **4**, which is the second most abundant species. The species **4** has the same charge as **2** and the difference in internal versus terminal preference between the two species can therefore not arise from electrostatic interactions alone. The difference in hydrogen-bonding capability between **2** and **4** may be invoked to explain why a larger quantity of internal GG adducts are produced with **4** than with **2**. It is known that OH^- has a high hydrogen-bonding donation capacity whereas Cl^- has none;[4] therefore **4** has better hydrogen-donating properties than **2**. Theoretical calculations on different possible transition states of the monofunctional adducts *cis*-$[PtCl(^{15}NH_3)_2\{N7G\}]^+$ (**2**-N7G) and *cis*-$[Pt(^{15}NH_3)_2(H_2O)\{N7G\}]^+$ (**3**-N7G) show that the transition state structures are largely determined by hydrogen bonding from Pt-ammine-hydrogen to O=C6 in the case of **2**-N7G, and by hydrogen bonding from Pt-aqua-hydrogen to O=C6 in **3**-N7G.[62] In **3**-N7G the transition-state energy is significantly lower than in **2**-N7G. In a kinetic study of the reaction between **2**/**3**/**4**/*cis*-$[Pt(^{15}NH_3)_3(H_2O)]^{2+}$ and double-stranded DNA the rate of platination for the four Pt complexes was found to decrease in the order **3** > **4** > *cis*-$[Pt(^{15}NH_3)_3(H_2O)]^{2+} \gg$ **2**.[63] This decrease in reactivity parallels the ability of the ligands of the Pt complexes to donate hydrogen bonds; $H_2O > OH > NH_3$, absent for Cl^-.[4]

Previous studies have shown that the 5′-G in GG steps is more readily platinated than the 3′-G.[7,10] It is therefore likely that it is the 5′-G of the terminal GG step that forms the monofunctional adduct with Pt^{II}. Other factors support this: 1) the *cis*-$[PtCl(^{15}NH_3)_2\{N7G_1\}]^+$ adduct is detected in the reaction starting with **1** and **II**, while the *cis*-$[PtCl(^{15}NH_3)_2\{N7G_2\}]^+$ adduct is not seen (from 2D $[^1H,^1H]$ NOESY NMR experiments), 2) the Zn^{II} and Mn^{II} titrations of **II** show that G_1 is preferred over G_2 (Figures 2b and 5), and 3) in **II** the 5′-G is much more accessible than the 3′-G, which has been shown to be of significant importance for the rate of platination.[7] Assuming that G_1 forms the monofunctional adduct with Pt^{II} in the terminal GG step, one

may rationalize that the internal GG step has a larger number of possible hydrogen-bonding sites than the terminal GG step, owing to the fact that it has neighbouring residues on both sides. Furthermore, other studies (see above) predict a stronger electrostatic potential in the central part of **II**.[14–19,54] This also induces a stronger hydrogen bonding capability of the internal GG step than the terminal guanine. From this it may be deduced that hydrogen-bonding capacity and electrostatic potential are relatively more important than steric effects in the binding mechanism of cisplatin to duplex DNA. It has also been indicated that the hydrogen-bonding donor ability of Pt^{II} am(m)ine complexes is crucial for their antitumour activity.[64]

Another explanation may be simply that it is the lack of a phosphate group on the 5′ side of the terminal guanine that makes this GG step less reactive than the internal GG step. This can be rationalized from the fact that several studies have shown that the rate of platination is increased when a phosphate group is introduced on the 5′ side of the guanine.[7,65–68] The enhanced rate of reaction has been explained by hydrogen bonding between the phosphate group and the Pt^{II} complex. Since **4** has a higher hydrogen-donating capacity than **2**, the lacking 5′-phosphate group on the terminal guanine will influence **4** more than **2**. Therefore, **4** has a higher preference for the internal GG step than **2**.

Conclusion

For the first time we present here the reactivity of a double-helical DNA oligonucleotide (**II**) containing both a terminal GG step and an internal GG step. By using natural-abundance 2D [^{1}H,^{15}N] HMBC we have unambiguously determined that Zn^{II} coordinates to G-N7 in **II**, with a high preference for the internal 5′-G, and to a less extent to the terminal 5′-G. The two 3′-Gs are significantly less metalated. The reactivity of Mn^{II} (paramagnetic) towards **II** was determined by ^{1}H line-broadening measurements, and Mn^{II} also preferentially binds to the internal 5′-G-N7. The preference of these two metal ions for the internal GG step indicates a higher negative electrostatic potential in the internal region of the duplex. This has previously been shown for single-stranded DNA oligonucleotides, and theoretical calculations have also suggested an increased electrostatic potential in the central part of duplex oligonucleotides.[14–19,54] We have also studied a duplex DNA oligonucleotide (**I**) containing a terminal GG step and an internal single G, this sequence shows exclusively Zn^{II} and Mn^{II} binding to the terminal 5′-G. A recent X-ray study of Co^{II}, Ni^{II}, and Zn^{II} binding to **I** found that all three of these metal ions coordinated exclusively to the terminal guanine,[22] and the authors concluded that these transition-metal ions generally do not bind to internal parts of B-DNA. We have previously shown that transition-metal ions usually react with the 5′-G in GG steps (never in a 5′-GC step), and we therefore believe that the reactivity of **I** may simply be explained from the fact that the terminal guanine is the only 5′-G in a GG step in **I**.

For comparison, we have also determined the binding preference of the Pt^{II} complexes *cis*-[PtCl($^{15}NH_3$)$_2$(H_2O)]$^+$ and *cis*-[Pt($^{15}NH_3$)$_2$(H_2O)(OH)]$^+$ towards **II** by using 1D/2D ^{1}H and 2D [^{1}H,^{15}N] HSQC NMR spectroscopy. These complexes react mainly with the internal GG step, forming the well known 1,2-GG crosslink. This shows that the selectivity of cisplatin is not as affected by steric effects as other authors have suggested;[5,7,55] instead, cisplatin reacts preferentially at the site where electrostatic effects or hydrogen-bonding abilities are optimized.

The conformation of the Zn^{II}/**II** adduct was investigated by 2D ^{1}H and ^{31}P NMR spectroscopy. Interestingly, the characteristic upfield shift of the H2′ signal (~0.5 ppm) on the 5′ neighbouring residues of intrastrand 1,2-GG cisplatin adducts was also observed for the Zn^{II}/**II** adduct. Furthermore, ^{31}P NMR spectroscopy of Zn^{II}/**II** showed a conformational change in the phosphodiester backbone of the duplex. Surprisingly, Zn^{II} monofunctional coordination to G-N7 may induce structural changes in the duplex similar to that observed for nonlabile Pt adducts, for example, the monofunctional *trans-EE*/duplex adduct.[50]

Experimental Section

Materials: ^{15}N-labeled cisplatin was prepared according to the published method.[69] The three oligonucleotides [d(GGCGCC)]$_2$ **I**, [d(GGTACCGGTACC)]$_2$ **II**, and [d(GGTATATATACCGGTATATATACC)]$_2$ **III** were purchased from DNA Technology A/S (Aarhus, DK) and obtained as crude products from ethanol precipitation. Acetonitrile, triethylammonium acetate buffer (made from equimolar amounts of triethylamine and acetic acid), and NaOH were purchased from Baker; sodium perchlorate, perchloric acid, and $MnCl_2$ from Merck, and $ZnCl_2$ from Aldrich (99.999% purity, to minimize the level of paramagnetic metal ion impurities).

Sample preparation: All weights were determined using an Ohaus Explorer Pro Analytical balance, repeatability 0.1 mg (Ohaus Corporation, US). The pH was measured by a Sentron Argus pH meter connected to a Sentron Red-line Standard pH probe, calibrated with pH 4.00 and 7.00 Sentron buffers.

The three oligonucleotides were purified by HPLC (Waters 626 LC instrument with Millennium 32 software) with an Xterra, MS C_{18}, 2.5 μm (Waters Corporation, US) column. Eluents used for HPLC were A: 5% acetonitrile in 0.1 M TEAA, B: 25% acetonitrile in 0.1 M TEAA, C: 30% acetonitrile in 0.1 M TEAA. The following 15 min linear gradients was used: 1) for **I**: 90% A and 10% B to 50% A and 50% B, 2) for **II**: 80% A and 20% C to 55% A and 45% C, and 3) for **III**: 50% A and 50% C to 20% A and 80% C. The flow rate in each case was 2.0 mL min^{-1} at ambient temperature. TEAA and acetonitrile were removed by freeze-drying the sample three times, first at neutral pH, then pH 3.3, and finally at pH 12.5.

Mn^{II} and Zn^{II} titrations: Mn^{II} and Zn^{II} titrations of the two oligonucleotides were carried out in NMR tubes by adding aliquots of the metal salt solutions (dissolved in D_2O) with a micropipette. The samples of the oligomers were dissolved in D_2O (pH 5.0–6.5, 10 mM phosphate buffer and 0–100 mM sodium perchlorate). The concentration of metal ions was increased in increments to maximum r values (r = [metal]/[duplex DNA]) in the range 5×10^{-4}–7×10^{-3} for the paramagnetic Mn^{II} system, and 1–60 for the diamagnetic Zn^{II} system.

^{31}P and ^{15}N natural-abundance NMR: 2D [^{1}H,^{15}N] HMBC and [^{1}H,^{31}P] HSQC were recorded for **II** with and without added Zn^{II} salt: 1) 0.29 mM **II** in 10 mM phosphate buffer, pH 5.0, 99.9% D_2O, and, 2) sample (1)

with a Zn^{II}/duplex ratio of 16.8. Sample (2) is the same as was used for the Zn^{II} titration at low salt concentration.

Reaction of cisplatin with II: All reactions were performed in 10% D_2O in H_2O. Duplex **II** was reacted both with ^{15}N-labelled *cis*-[$PtCl_2(^{15}NH_3)_2$] (**1**) and with *cis*-[$Pt(^{15}NH_3)_2(H_2O)_2$] (**3**). The reactions between **1** and **II** were performed at ratios of 1:1 and 1:2, respectively, while in the reaction with **3** a 1:1 ratio was used. Reaction conditions for samples containing **1**; 0.1 M $NaClO_4$, pH 6.0, 298 K, and, samples containing **3**; 0.1 M $NaClO_4$, pH 6.4 (pH increased to a final value of 8.2 during the reaction), and 285 K. The reactions were followed by 2D [^1H,^{15}N] HSQC and 1D ^1H NMR spectroscopy.

The peak volumes in the 2D [^1H,^{15}N] HSQC NMR spectra were measured using the integration routines in the NMR software. The rate constants for the reactions were determined by a nonlinear optimization procedure using the program SCIENTIST (version 2.01, Micromath Scientific Software, Salt Lake City, USA).

NMR Spectroscopy: NMR experiments were performed on the following instruments: Bruker UltraShield 500 MHz with a triple resonance TXI probe head and a Bruker AVANCE 600 MHz with triple resonance CryoProbe (TCI for ^{15}N detection and HPC for ^{31}P). The 500 MHz instrument was used for the acquisition of 2D [^1H,^{15}N] HSQC and ^1H 1D/2D NMR spectra, while 2D [^1H,^{15}N] HMBC, 2D [^1H,^{31}P] HSQC and ^1H 1D/2D were recorded on the 600 MHz instrument. The 2D HSQC[70–72] spectra were phase-sensitive using the Echo/Antiecho-TPPI quadrature detection scheme, while 2D HMBC[73] was recorded in magnitude mode. Pulsed-field gradients were applied to select the proper coherence. Delays were optimized according to the following: 2D [^1H,^{15}N] HSQC ($^1J_{NH}$ = 72 Hz), 2D [^1H,^{15}N] HMBC ($^2J_{NH}$ = 12 Hz) and 2D [^1H,^{31}P] HSQC (J_{PH} = 10 Hz). The following parameters were used: 2D [^1H,^{15}N] HMQC; spectral width in *F*1 1418 Hz and in *F*2 8013 Hz, 2048 complex points in each FID in t_2 and 64 increments in t_1, 4–32 transients averaged for each increment and relaxation delay of 2 s, 2D [^1H,^{15}N] HMBC; spectral width in *F*1 6083 Hz and in *F*2 7183 Hz, 2048 complex points in each FID in t_2 and 70–86 increments in t_1, 764–1024 transients averaged for each increment and relaxation delay of 2 s, 2D [^1H,^{31}P] HSQC; spectral width in *F*1 1214 Hz and in *F*2 7211 Hz, 1024 complex points in each FID in t_2 and 96–128 increments in t_1, 200–280 transients averaged for each increment and relaxation delay of 1.5 s. ^1H NMR spectra were referenced to 3-trimethylsilyl-2,2′,3,3′-tetradeuteropropionate (TSP) set to 0 ppm, ^{15}N NMR spectra to 1.0 M ^{15}N-enriched NH_4Cl in 1.0 M HCl solution (0 ppm), and ^{31}P NMR spectra to trimethyl phosphate (TMP) set to 0 ppm. The NMR data were processed using the program XWIN-NMR Version 2.6 or TopSpin Version 1.3. The t_1 FIDs in the 2D NMR data sets were linearly predicted to four times their original value. Analysis of 2D spectra was performed by using the program Sparky, Version 3.111 (UCSF).

Acknowledgements

We thank the Centre of Pharmacy (University of Bergen) for financial support, and Dr. Helena Kovacs (Bruker BioSpin) for NMR spectroscopy assistance.

[1] V. K. Misra, D. E. Draper, *Biopolymers* **1998**, *48*, 113–135.
[2] V. K. Misra, D. E. Draper, *Proc. Natl. Acad. Sci. USA* **2001**, *98*, 12456–12461.
[3] H. Strehlow, *Rapid Reactions in Solution*, VCH, Weinheim, **1992**, p. 116.
[4] C. B. Black, J. A. Cowan, *J. Am. Chem. Soc.* **1994**, *116*, 1174–1178.
[5] R. Lavery, A. Pullman, *Biophys. Chem.* **1984**, *19*, 171–181.
[6] K. W. Kohn, J. A. Hartley, W. B. Mattes, *Nucleic Acids Res.* **1987**, *15*, 10531–10549.
[7] V. Monjardet-Bas, M.-A. Elizondo-Riojas, J.-C. Chottard, J. Kozelka, *Angew. Chem.* **2002**, *114*, 3124–3127; *Angew. Chem. Int. Ed.* **2002**, *41*, 2998–3001.
[8] N. A. Froeystein, J. T. Davis, B. R. Reid, E. Sletten, *Acta Chem. Scand.* **1993**, *47*, 649–657.
[9] E. Moldrheim, B. Andersen, N. A. Froystein, E. Sletten, *Inorg. Chim. Acta* **1998**, *273*, 41–46.
[10] J. Vinje, J. A. Parkinson, P. J. Sadler, T. Brown, E. Sletten, *Chem. Eur. J.* **2003**, *9*, 1620–1630.
[11] I. Saito, M. Takayama, H. Sugiyama, K. Nakatani, A. Tsuchida, M. Yamamoto, *J. Am. Chem. Soc.* **1995**, *117*, 6406–6407.
[12] I. Saito, K. Nakatani, *Bull. Chem. Soc. Jpn.* **1996**, *69*, 3007–3019.
[13] I. Saito, T. Nakamura, K. Nakatani, *J. Am. Chem. Soc.* **2000**, *122*, 3001–3006.
[14] M. C. Olmsted, C. F. Anderson, M. T. Record, *Proc. Natl. Acad. Sci. USA* **1989**, *86*, 7766–7770.
[15] W. Zhang, J. P. Bond, C. F. Anderson, T. M. Lohman, M. T. Record, *Proc. Natl. Acad. Sci. USA* **1996**, *93*, 2511–2516.
[16] W. Zhang, H. Ni, M. W. Capp, C. F. Anderson, T. M. Lohman, M. T. Record Jr., *Biophys. J.* **1999**, *76*, 1008–1017.
[17] M. C. Olmsted, J. P. Bond, C. F. Anderson, M. T. Record Jr., *Biophys. J.* **1995**, *68*, 634–647.
[18] V. M. Stein, J. P. Bond, M. W. Capp, C. F. Anderson, M. T. Record Jr., *Biophys. J.* **1995**, *68*, 1063–1072.
[19] J. D. Ballin, I. A. Shkel, M. T. Record Jr., *Nucleic Acids Res.* **2004**, *32*, 3271–3281.
[20] S. Snygg Ase, M. Brindell, G. Stochel, K. C. Elmroth Sofi, *Dalton Trans.* **2005**, 1221–1227.
[21] A. Sykfont, A. Ericson, S. K. C. Elmroth, *Chem. Commun.* **2001**, 1190–1191.
[22] S. L. Labiuk, L. T. J. Delbaere, J. S. Lee, *J. Biol. Inorg. Chem.* **2003**, *8*, 715–720.
[23] S. O. Ano, Z. Kuklenyik, L. G. Marzilli, *Cisplatin* **1999**, 247–291.
[24] J. H. J. den Hartog, C. Altona, J. H. van Boom, G. A. van der Marel, C. A. G. Haasnoot, J. Reedijk, *J. Biomol. Struct. Dyn.* **1985**, *3*, 1137–1155.
[25] F. Herman, J. Kozelka, V. Stoven, E. Guittet, J.-P. Girault, T. Huynh-Dinh, J. Igolen, J.-Y. Lallemand, J.-C. Chottard, *Eur. J. Biochem.* **1990**, *194*, 119–133.
[26] D. Yang, S. S. G. E. van Boom, J. Reedijk, J. H. van Boom, A. H.-J. Wang, *Biochemistry* **1995**, *34*, 12912–12920.
[27] A. Gelasco, S. J. Lippard, *Biochemistry* **1998**, *37*, 9230–9239.
[28] S. U. Dunham, S. U. Dunham, C. J. Turner, S. J. Lippard, *J. Am. Chem. Soc.* **1998**, *120*, 5395–5406.
[29] J. A. Parkinson, Y. Chen, Z. Guo, S. J. Berners-Price, T. Brown, P. J. Sadler, *Chem. Eur. J.* **2000**, *6*, 3636–3644.
[30] L. G. Marzilli, J. S. Saad, Z. Kuklenyik, K. A. Keating, Y. Xu, *J. Am. Chem. Soc.* **2001**, *123*, 2764–2770.
[31] S. J. Berners-Price, T. A. Frenkiel, U. Frey, J. D. Ranford, P. J. Sadler, *J. Chem. Soc. Chem. Commun.* **1992**, 789–791.
[32] S. J. Berners-Price, P. J. Sadler, *Coord. Chem. Rev.* **1996**, *151*, 1–40.
[33] H. Sigel, B. Song, *Met. Ions Biol. Syst.* **1996**, *32*, 135–205.
[34] H. Sigel, E. M. Bianchi, N. A. Corfu, Y. Kinjo, R. Tribolet, R. B. Martin, *Chem. Eur. J.* **2001**, *7*, 3729–3737.
[35] C. P. Da Costa, H. Sigel, *Inorg. Chem.* **2003**, *42*, 3475–3482.
[36] V. Sychrovsky, J. Sponer, P. Hobza, *J. Am. Chem. Soc.* **2004**, *126*, 663–672.
[37] G. W. Buchanan, J. B. Stothers, *Can. J. Chem.* **1982**, *60*, 787–791.
[38] G. Wang, B. L. Gaffney, R. A. Jones, *J. Am. Chem. Soc.* **2004**, *126*, 8908–8909.
[39] M. Soler-Lopez, L. Malinina, V. Tereshko, V. Zarytova, J. A. Subirana, *J. Biol. Inorg. Chem.* **2002**, *7*, 533–538.
[40] N. G. A. Abrescia, T. Huynh-Dinh, J. A. Subirana, *J. Biol. Inorg. Chem.* **2002**, *7*, 195–199.
[41] Y. G. Gao, M. Sriram, A. H. J. Wang, *Nucleic Acids Res.* **1993**, *21*, 4093–4101.
[42] M. D. Reily, L. G. Marzilli, *J. Am. Chem. Soc.* **1986**, *108*, 8299–8300.
[43] C. S. Fouts, L. G. Marzilli, R. A. Byrd, M. F. Summers, G. Zon, K. Shinozuka, *Inorg. Chem.* **1988**, *27*, 366–376.
[44] J. Kozelka, G. Barre, *Chem. Eur. J.* **1997**, *3*, 1405–1409.
[45] R. N. Bose, L. L. Slavin, J. W. Cameron, D. L. Luellen, R. E. Viola, *Inorg. Chem.* **1993**, *32*, 1795–1802.

[46] R. N. Bose, R. E. Viola, R. D. Cornelius, *J. Am. Chem. Soc.* **1984**, *106*, 3336–3343.
[47] L. L. Slavin, R. N. Bose, *J. Chem. Soc. Chem. Commun.* **1990**, *18*, 1256–1258.
[48] V. L. Pecoraro, J. D. Hermes, W. W. Cleland, *Biochemistry* **1984**, *23*, 5262–5271.
[49] M.-A. Elizondo-Riojas, J. Kozelka, *J. Mol. Biol.* **2001**, *314*, 1227–1243.
[50] B. Andersen, N. Margiotta, M. Coluccia, G. Natile, E. Sletten, *Met.-Based Drugs* **2000**, *7*, 23–32.
[51] C. J. Van Garderen, C. Altona, J. Reedijk, *Inorg. Chem.* **1990**, *29*, 1481.
[52] V. Brabec, J. Reedijk, M. Leng, *Biochemistry* **1992**, *31*, 12397–12402.
[53] R. Zaludova, V. Kleinwachter, V. Brabec, *Biophys. Chem.* **1996**, *60*, 135–142.
[54] R. Lavery, B. Pullman, *Int. J. Quantum Chem.* **1981**, *20*, 259–272.
[55] S. Furois-Corbin, B. Pullman, R. Lavery, *Int. J. Quantum Chem. Quantum Biol. Symp.* **1984**, *11*, 273–286.
[56] M. A. Jakupec, M. Galanski, B. K. Keppler, *Rev. Physiol. Biochem. Pharmacol.* **2003**, *146*, 1–53.
[57] J. Reedijk, *Proc. Natl. Acad. Sci. USA* **2003**, *100*, 3611–3616.
[58] J. Vinje, F. P. Intini, G. Natile, E. Sletten, *Chem. Eur. J.* **2004**, *10*, 3569–3578.
[59] D. P. Bancroft, C. A. Lepre, S. J. Lippard, *J. Am. Chem. Soc.* **1990**, *112*, 6860–6871.
[60] N. P. Johnson, J. D. Hoeschele, R. O. Rahn, *Chem. Biol. Interact.* **1980**, *30*, 151–159.
[61] W. Schaller, H. Reisner, E. Holler, *Biochemistry* **1987**, *26*, 943–950.
[62] M. H. Baik, R. A. Friesner, S. J. Lippard, *J. Am. Chem. Soc.* **2003**, *125*, 14082–14092.
[63] F. Legendre, V. Bas, J. Kozelka, J.-C. Chottard, *Chem. Eur. J.* **2000**, *6*, 2002–2010.
[64] C. G. Van Kralingen, J. Reedijk, *Cienc. Biol.* **1980**, *5*, 159–161.
[65] T. W. Hambley, *J. Chem. Soc. Dalton Trans.* **2001**, 2711–2718.
[66] A. B. Robins, *Chem. Biol. Interact.* **1973**, *6*, 35–45.
[67] A. T. M. Marcelis, C. Erkelens, J. Reedijk, *Inorg. Chim. Acta* **1984**, *91*, 129–135.
[68] J.-P. Girault, J.-C. Chottard, G. Chottard, J.-Y. Lallemand, *Biochemistry* **1982**, *21*, 1352–1356.
[69] J. S. Kerrison, P. J. Sadler, *J. Chem. Soc. Chem. Commun.* **1977**, 861–863.
[70] A. G. Palmer III, J. Cavanagh, P. E. Wright, M. Rance, *J. Magn. Reson.* **1991**, *93*, 151–170.
[71] L. E. Kay, P. Keifer, T. Saarinen, *J. Am. Chem. Soc.* **1992**, *114*, 10663–10665.
[72] J. Schleucher, M. Schwendinger, M. Sattler, P. Schmidt, O. Schedletzky, S. J. Glaser, O. W. Sorensen, C. Griesinger, *J. Biomol. NMR* **1994**, *4*, 301–306.
[73] A. Bax, M. F. Summers, *J. Am. Chem. Soc.* **1986**, *108*, 2093–2094.

Received: June 24, 2005
Published online: October 6, 2005

